

**ANNUAL MONITORING OF REPRODUCTIVE  
TRAITS OF FEMALE YELLOWFIN TUNA  
(*THUNNUS ALBACARES*) IN THE EASTERN ATLANTIC OCEAN**

N.C. Diaha<sup>1</sup>, I. Zudaire<sup>2,3</sup>, E. Chassot<sup>4</sup>, B.D. Barrigah<sup>1</sup>, Y.D. Irié<sup>1</sup>, D.A. Gbeazere<sup>5</sup>,  
D. Kouadio<sup>5</sup>, C. Pecoraro<sup>2,6</sup>, M.U. Romeo<sup>6</sup>, H. Murua<sup>7</sup>, M.J. Amandè<sup>1</sup>, P. Dewals<sup>5</sup>, N. Bodin<sup>4</sup>

SUMMARY

*The reproductive biology of female yellowfin tuna (Thunnus albacares; YFT) was studied through the estimation of some important traits: sex-ratio, size at maturity (L<sub>50</sub>), spawning seasonality, fish condition and fecundity, in the Eastern Atlantic Ocean through a routine monitoring sampling carried out from February 2014 to April 2015. A total of 1483 (704 females and 779 males) YFT was collected on a weekly sampling at the fishing port of Abidjan, and ovaries of 527 females (76.4-166 cm F<sub>L</sub>) were analyzed for histology. A high reproductive activity of females was observed during boreal winter (December to April), being significantly active in December-January. L<sub>50</sub> was estimated at 99.2 cm F<sub>L</sub>. Condition index analysis during the spawning season did not show a clear pattern on energy allocation strategy for reproduction. However, the assessment of gonadosomatic (GSI) and hepatosomatic (HIS) indices during the ovarian development described an accumulative pattern with the highest values in spawning females. Mean batch fecundity was estimated at 2.91±1.22 million oocytes and mean relative batch fecundity at 54.39±22.05 oocytes per fish gram.*

RÉSUMÉ

*La biologie reproductive des femelles d'albacore (Thunnus albacares ; YFT) a été étudiée par le biais de l'estimation de certaines caractéristiques importantes : sex-ratio, taille à maturité (L<sub>50</sub>), caractère saisonnier du frai, état du poisson et fécondité dans l'océan Atlantique Est par un échantillonnage de suivi habituel effectué de février 2014 à avril 2015. Au total, 1.483 albacores (704 femelles et 779 mâles) ont été prélevés sur un échantillonnage hebdomadaire au port de pêche d'Abidjan, et les ovaires de 527 femelles (76,4-166 cm FL) ont été analysés pour déterminer l'histologie. Une forte activité de reproduction des femelles a été observée au cours de l'hiver boréal (de décembre à avril), en nette activité entre décembre et janvier. L<sub>50</sub> était estimée à 99,2 cm FL. L'analyse de l'indice de condition pendant la saison de frai n'a pas dégagé de tendance claire sur la stratégie de répartition de l'énergie pour la reproduction. Toutefois, l'évaluation des indices gonadosomatiques (GSI) et hépatosomatiques (HIS) au cours du développement ovarien décrivait un schéma cumulatif dont on trouvait les valeurs les plus élevées chez les femelles reproductrices. La moyenne de la fécondité par acte de ponte a été estimée à 2,91±1,22 millions d'ovocytes et la moyenne relative de la fécondité par acte de ponte à 54,39±22,05 des ovocytes par gramme de poisson.*

RESUMEN

*Se estudió la biología reproductiva de hembras de rabil (Thunnus albacares, YFT) mediante la estimación de algunos rasgos importantes, como la ratio de sexos, la talla por madurez (L<sub>50</sub>), la estacionalidad del desove, la condición de los peces y la fecundidad, en el océano Atlántico oriental mediante un muestreo rutinario de seguimiento desde febrero de 2014 hasta abril de 2015. Un total de 1483 rabiles (704 hembras y 779 machos) fue recogido en un muestreo*

<sup>1</sup> Centre de Recherches Océanologiques 29 Rue des Pêcheurs, B.P. V 18 Abidjan, Côte d'Ivoire

<sup>2</sup> Institut de Recherche pour le Développement (IRD) - UMR 248 MARBEC CNRS/Ifremer/IRD/UM, Av. Jean Monnet, BP 171, 34200 Sète, France

<sup>3</sup> IKERBASQUE, Basque Foundation for Science, Maria Diaz de Haro 3, 48013 Bilbao, Spain

<sup>4</sup> Institut de Recherche pour le Développement (IRD) - UMR 248 MARBEC CNRS/Ifremer/IRD/UM, SFA, Fishing Port, B570, Victoria, Seychelles

<sup>5</sup> Institut de Recherche pour le Développement (IRD) - UMR 248 MARBEC CNRS/Ifremer/IRD/UM, Observatoire Thonier, IRD 15 BP 917 Abidjan 15, Côte d'Ivoire

<sup>6</sup> Dept. Biological, Geological & Environmental Sciences (BiGeA), University of Bologna, Via S. Alberto 163, 48123 Ravenna, Italy

<sup>7</sup> AZTI, Marine Research Division, Herrera Kaia-Portu aldea z/g, 20110 Pasaia, Spain

semanal en el puerto pesquero de Abiyán, y se analizaron para su histología ovarios de 527 hembras (76,4-166 cm  $F_L$ ). Durante el invierno boreal (diciembre a abril) se observó una elevada actividad reproductiva de las hembras, siendo especialmente activas en diciembre-enero.  $L_{50}$  se estimó en 99,2 cm  $F_L$ . El análisis del índice de condición durante la temporada de desove no mostró un patrón claro de la estrategia de asignación de energía para la reproducción. Sin embargo, la evaluación de los índices gonadosomático (GSI) y hepatosomático (HIS) durante el desarrollo de los ovarios describía un patrón acumulativo con los mayores valores en las hembras reproductoras. La fecundidad media por lote se estimó en  $2,91 \pm 1,22$  millones de oocitos y la fecundidad media relativa por lote en  $54,39 \pm 22,05$  oocitos por gramo de pez.

#### KEYWORDS

*Reproductive behaviour, Sex ratio, Sexual maturity, Condition index, Yellowfin Tuna, Atlantic Ocean*

## 1. Introduction

Monitoring reproductive traits of highly exploited fish species, like tropical tunas, provides useful information to better understand the fluctuations of population dynamic and how these changes could affect population resilience to fishing and environmental changes (Murua and Motos 2006; Morgan *et al.* 2009). Although traditionally used as biological indicator of stock viability in stock/recruitment relationships, spawning stock biomass (SSB), has been shown not to be the most appropriate parameter for estimating stock productivity (Marshall *et al.* 1998; Marshall 2009; Kell *et al.* 2015) since it does not take into account properly different size/age dependent fecundity. Some of the reproductive traits involved in recruitment dynamics are considered highly plastic, e.g., fecundity, size at maturity, spawning duration (Morgan 2008), and thus, traditionally applied methods could fail in explaining large part of that variability (Williams and Shertzer 2003). Therefore, it is important to monitor these reproductive traits so as to include their variability when estimating population productivity (Trippel 1999; Morgan *et al.*, 2009).

Yellowfin tuna (*Thunnus albacares*; YFT), is a large epipelagic species widely distributed in tropical and subtropical regions (Collette and Nauen, 1983). It is a high value species extensively exploited by different fishing methods worldwide. Tuna purse-seine (PS) fishery is the main fishing gear corresponding to more than 80% of the total annual catch of YFT in the Eastern Atlantic Ocean (ICCAT 2013). Two different fishing modes resulting in different size and species composition of the catch are used by the PS fleet (Joseph 2003): Fish Aggregating Devices (FADs) and Free-Swimming Schools (FSC) of tuna. In the last decade, YFT mean annual catches represented 60,000 tons (t) from which around 30-40% were caught on FADs in the Eastern Atlantic Ocean (Delgado *et al.* 2014; Chassot *et al.* 2015). Reproductive studies on YFT were carried out previously in the Eastern (Albaret *et al.* 1976; Albaret 1977; Bard and Capisano 1991; Capisano and Fonteneau 1991), and Western Atlantic Ocean (Arocha *et al.* 2001; Zavala-Camin 1977), as well as in the Pacific Ocean (Orange 1961; McPherson 1991; Schaefer 1996; Schaefer 1998). However, updated information is required to better assess the high variability of some of these important parameters as recently done in the Indian Ocean (Zhu *et al.* 2008; Zudaire *et al.* 2013a; Zudaire *et al.* 2013b).

Thus, the overarching objectives of this work are to assess the main reproductive traits (sex-ratio, size at maturity, spawning seasonality, fish condition and fecundity) and length-weight relationships of yellowfin tuna in the Eastern Atlantic Ocean based on an all-year round sampling. The monitoring of these reproductive traits will contribute to the knowledge of basic parameters for the study of YFT population dynamics.

## 2. Material and methods

### 2.1 Field sampling

Around 30 YFT caught by the purse-seine fleet operating in the eastern Atlantic Ocean (**Figure 1**), were sampled monthly at the “Pêche et Froid” cannery of the fishing port of Abidjan from February 2014 to April 2015. Each fish was sexed and measured for fork length ( $F_L$ ; cm), first dorsal length ( $FDL$ ; cm), thorax length ( $TL$ ; cm) and total weight (kg). Ovaries and liver were removed and weighted to the nearest g. A portion from each end and midsection of one gonad lobe of each fish was immersed in 4% buffered formaldehyde for subsequent histological analysis. Fish traceability regarding, vessel name, fishing date and area, sea surface temperature, and fishing mode (FADs and FSC), was obtained through vessels logbooks.

## 2.2 Length-weight relationships and sex ratio

Multiple linear regression model was applied on the overall sampled YFT (males and females) to assess the variability observed in weight as the function of length and sex. Sex ratio (SR) was calculated as the proportion of females by 5 cm  $F_L$  classes, and chi square tests were used to examine differences from an expected 1:1 by size class

$$SR = \frac{N_f}{N_t} \times 10^2$$

Where  $N_f$  is the number of females and  $N_t$  is the total number of sampled fish.

## 2.3 Condition indices

Fish condition was evaluated by applying three conditions indices, i.e. the gonadosomatic index (GSI), the hepatosomatic index (HSI) and the condition factor (K) following:

$$GSI = \frac{W_g}{W} \times 10^2$$

$$HSI = \frac{W_l}{W} \times 10^2$$

$$K = \frac{W}{F_L^3} \times 10^2$$

where  $W_g$  is fish gonad-free weight (g),  $W$  is total fish weight (g), and  $W_l$  is the liver weight (g). Variations of the three condition indices were analyzed according to month and maturity development phase.

## 2.4 Histological analysis

A 1cm cross-section from the preserved portion of each ovary was embedded in paraffin, sectioned at 5-7  $\mu\text{m}$  and stained with H&E as described by (Constance 2015). Ovaries were classified according to the most advanced oocyte stage present (Zudaire et al. 2013a): (i) immature phase ( $P_I$ ) which includes oocytes in the primary growth stage; (ii) developing phase ( $P_D$ ) which includes oocytes in the stages of cortical alveoli and primary and secondary vitellogenesis; (iii) spawning-capable phase ( $P_{SC}$ ) which includes oocytes in the stages of tertiary vitellogenesis, germinal vesicle migration and hydration; (iv) regressing phase ( $P_{RG}$ ); and (v) regenerating phase ( $P_R$ ) characterized by the presence of maturity makers, late-stage atresia and a thicker ovarian wall than seen in immature fish. The atretic condition to appraise the regressing phase was based on the method of Hunter and Macewicz (1985). However, the estimation of atresia for ovaries collected at the cannery entails difficulties due to their exposure to the brine conservation process used in PS. This conservation method produces breakages in the follicle wall and chorion and, hence, precise quantification of atresia was not always possible.

## 2.5 Oocyte size-frequency distribution

16 ovaries covering the eight oocyte development stages were selected for oocyte size-frequency distribution analysis. From each preserved portion of ovary, a 0.04g ( $\pm 0.0001\text{g}$ ) sample was removed, placed into a 125- $\mu\text{m}$  sieve and sprayed with high pressure water in order to separate the oocytes from connective tissue. Oocytes were then collected in a Petri dish in order to be photographed with a digital camera. Subsequently, the number and size of all oocytes were determined on each image using ImageJ analysis software.

## 2.6. Length at 50% maturity

$L_{50}$  (i.e., size at which 50% of the population is mature) was calculated by fitting the proportion of mature females (identified through histological analysis) by 5 cm  $F_L$  classes to a logistic equation (Saborido-Rey and Junquera 1998) (Ashton, 1972):

$$P_{\text{mature}} = e^{\alpha+\beta L}/1+e^{\alpha+\beta L}$$

where  $P_{\text{mature}}$  = the predicted proportion of mature females;  $L$  = the  $F_L$  in cm; and  $\alpha$  and  $\beta$  are the coefficients of the logistic equation.

The  $L_{50}$  was estimated as the ratio of the coefficients ( $-\alpha \times \beta^{-1}$ ). A non-linear regression (the Marquardt method without restrictions; Marquardt 1963) was used to fit the logistic equation to the data. The maturity curve was fitted to the data on the basis of two different assumptions regarding female maturity threshold: (i) females with ovaries at the cortical alveolar stage onward (Brown-Peterson et al. 2011) and (ii) females with ovaries at advanced vitellogenic oocytes were considered mature (Schaefer 1998; Zhu *et al.* 2008).

### 2.7 Fecundity estimation

Batch fecundity (BF), i.e., the total number of oocytes released per batch, was estimated for 80 ovaries by gravimetric method (Hunter *et al.*, 1989), counting the germinal vesicle migration or hydration stage oocytes present in the ovary. Homogeneity in oocyte density among whole ovary was assumed on the basis of previous works on tuna (Stéquert and Ramcharrun 1996). For BF analyses, three subsamples of 0.1 g ( $\pm 0.01$ ) were collected from each ovary. Each subsample was saturated with glycerin and oocytes were counted under a stereomicroscope (Schaefer 1998). Batch fecundity was calculated as the weighted mean density of the three subsamples multiplied by the total weight of the ovary. A threshold of 10% for the coefficient of variance was applied for the three subsamples, and when this threshold was surpassed, more subsamples were counted until this value was reached. Relative batch fecundity (BF<sub>rel</sub>) was estimated dividing the BF by fish gonad-free weight.

## 3. Results

### 3.1 Length-weight relationships and sex ratio

A total of 1,483 YFT, 704 females and 779 males, were sampled in the Eastern Atlantic Ocean between February 2014 and April 2015. Sex did not significantly affect the relationship between fork length and weight (p-value = 0.565). The results combining values of both sex showed a mean length-weight curve in accordance to that currently in use within ICCAT (Caverivière 1976), although the predicted weights were a bit higher for lengths larger than 120  $F_L$  (**Figure 2**).

The sex ratio of YFT did not differ significantly from 1:1 at small and intermediate size. In contrast, males were dominant at larger sizes (from 144 to 172 cm  $F_L$ ) (p-values < 0.05; **Table 1** and **Figure 3**).

### 3.2 Oocyte size-frequency distribution

The oocyte size frequency distribution at different ovarian developmental phases from the immature to the spawning capable phase was continuous without any gap in diameter between primary and secondary growth oocytes (**Figure 4**). A gap in diameter at around 470  $\mu\text{m}$  at tertiary vitellogenic stage (Vtg 3) and germinal vesicle migration stage (GVM) separated the pool of less developed oocytes from the largest modal group of oocytes forming a batch which was clearly separated during the germinal vesicle break down (GVBD) stage at around 490  $\mu\text{m}$ . At the hydration stage, the oocytes increased in size to above 950  $\mu\text{m}$ .

### 3.3 Length at 50% maturity

$L_{50}$  was estimated at 99.2 cm  $F_L$  for eastern Atlantic YFT when females with ovaries at the CA stage and onward were considered mature. This estimate increased to 124.6 cm  $F_L$  when the second criterion was applied, i.e., when the maturity threshold was defined as the presence of advanced vitellogenic oocytes (**Figure 5**).

### 3.4 Reproductive analysis

Histological analysis of YFT ovaries revealed an asynchronous ovarian development in which all oocyte stages were observed, without a dominant population present. The microscopic description of each of the different oocyte development stage is given in **Table 2**.

### 3.5 Spawning seasonality

According to the classification summarized in the **Table 2**, 21.5 % of YFT females were at immature phase, 35.6 % were at developing phase, 32.8 % were at spawning capable phase, 4.4 % at regressing phase, and finally 5.6 % showed ovaries at regenerating (**Table 3**). Moreover, 78.5 % of YFT females were mature, and 68.4% mature active. The highest proportion of females with ovaries at spawning capable phase was recorded from December to April, whereas females with less developed ovaries (i.e., immature and developing) were dominant from May to August (**Figure 6**).

### 3.6 Condition Indices

The analysis of the seasonal development of condition indices (**Figure 7**) in YFT females showed a period of high mean GSI values; from November ( $2.08 \pm 0.52$ ) to April ( $2.22 \pm 1.58$ ) with values higher than 1.5. During the following months, from May ( $0.31 \pm 0.12$ ) to September ( $0.58 \pm 0.27$ ), the GSI values decreased sharply and remained at low values (around 0.31).

K values remained almost constant through the spawning period, around  $1.92 \pm 0.01$ . However, a different development pattern of HSI values was observed between sexes during the spawning season. In females, the mean HSI values followed the GSI pattern, being HSI high from December ( $0.97 \pm 0.17$ ) to April ( $0.90 \pm 0.27$ ) and afterwards performing a decrease from May ( $0.61 \pm 0.19$ ) to August ( $0.68 \pm 0.11$ ).

The variability of GSI values at each ovary development phase is shown in **Figure 8**. The variability of GSI values at most developed ovaries is wider and there is an increase of GSI values as the ovary develops. Spawning capable females showed the highest mean GSI values ( $2.39 \pm 1.01$ ). In the case of GSI values for these stages were found over 1.5. HSI followed the GSI trend increasing as ovary develops describing the highest values at spawning capable phase females ( $1.00 \pm 0.20$ ). Regarding K values it was observed a decreasing pattern as ovary develops, with the lowest mean K value for spawning females ( $1.91 \pm 0.01$ ). However, no clear temporal pattern in K was observed (**Figure 8**).

### 3.7 Fecundity estimation

The estimated mean BF was  $2.91 \pm 1.22$  million oocytes and varied from 0.78 million to 7.56 million oocytes. The estimated mean BF<sub>rel</sub> was  $54.39 \pm 22.05$  oocytes per gram of gonad-free weight and fluctuated between 14.66 and 125.67 oocytes per gram of gonad-free weight. The BF appeared to be highly variable by month, making it difficult to identify a clear pattern for female fecundity. A maximum mean BF values was found in April ( $4.21 \pm 1.72$  million) and the minimum in January ( $2.62 \pm 0.98$  million), nevertheless, the analysis of variance (ANOVA) performed on the BF estimates by month did not reveal any significant differences between months at a 95% confidence level (ANOVA;  $F_{(5,80)}=0.846$ ,  $P=0.361$ ).

## 4. Discussion and future perspectives

The present study described a significant predominance of YFT males for specimen larger than 150 cm as shown by Capisano and Fonteneau (1991) in the same region. The predominance of male YFT at large sizes was also reported in the other oceans (Timohina and Romanov 1996; Schaefer 1998). On the contrary, the female dominant pattern described for the Atlantic Ocean (125-140 cm; Capisano and Fonteneau 1991) was not observed in our results. The difference of sex-ratio distribution by size is likely related to the sexual dimorphism in growth in YFT (Eveson *et al.* 2015), and/or sex differences in natural mortality.

A continuous oocyte size-frequency distribution was observed throughout different ovary maturation phases; which is in agreement with a previous report in the Pacific (Schaefer 1998) and Indian (Zudaire *et al.* 2013a) oceans. The continuous oocyte size frequency without any gap in the diameter between primary and secondary growth oocytes in different spawning phases as well as in different months has been considered as a sign of indeterminate fecundity (West 1990), as it may indicate the existence of a continuous recruitment of primary growth oocytes during the spawning season (Murua and Saborido-Rey 2003).

Size at maturity of YFT were estimated at 99.2 cm  $F_L$  and 124.6 cm  $F_L$  when maturity threshold is set at cortical alveoli and advanced vitellogenic stage, respectively. Previous studies applying both maturity thresholds in YFT in the Indian Ocean (Zudaire *et al.* 2013b) have shown very different values of 75 cm  $F_L$  and 103 cm  $F_L$ , respectively. However, previous studies in the Atlantic Ocean have observed similar results considering that between 100 and 110 cm FL all females were mature (Albaret 1977). The values obtained in the present work are more similar to the values obtained by macroscopic identification of ovary maturity which has been described as less accurate.

The assessment of the seasonal development of gonads and variations of GSI confirmed that YFT from Eastern Atlantic Ocean mainly spawn during boreal winter from November to April (ICCAT, 2011). Zudaire *et al.* (2013) suggested that the protracted spawning season and population asynchronicity in spawning activity of YFT could mask temporal variations in energy allocation analyzed by the study of condition indices throughout the spawning season (Zudaire *et al.* 2013b). Therefore, the assessment of energy reserve variations by female and male maturity phases is required in order to study the energetic dynamic cycle in individuals undergoing gonad development and reproductive activity. Our results showed that in female YFT the GSI and HSI followed a similar increasing trend as ovary develops.

Estimated mean batch fecundity (2.89 million oocytes) observed in the present work is very similar to the ones previously described by (Arocha *et al.* 2001) for the Western Atlantic Ocean, and by (Schaefer 1998) and (Itano 2000) for Eastern and Equatorial Western Pacific Ocean.

### Acknowledgments

We are grateful to Bernard Pintor, Abbas Khachab and all staff of « Pêche et Froid » for helpful assistance during sampling operations. The work was funded by IRD, the European Data Collection Framework (DCF, Reg 199/2008 and 665/2008) and the French *Direction des Pêches Maritimes et de l'Aquaculture* (DPMA). IZ was funded through a grant of the Ikerbasque Fundazioa and benefited from co-funding by IRD. CD benefited from a grant of ICCAT for training sessions at AZTI-Tecnalia and at the Seychelles Fishing Authority (SFA). We thank very much Maria Cedras (SFA) and Dr. Maria Korta (AZTI) for assistance in histological analyses. This work also benefited from the French ANR-funded project EMOTION (ANR JSV7 007 01).

### References

- Albaret, J. 1977. La reproduction de l'albacore (*Thunnus albacares*) dans le Golfe de Guinée. *Cash ORSTOM Sér Océan* 15:389–419.
- Albaret, J.J., Caverivière, A., Suisse de Sainte-Claire, E. 1976. Périodes et zones de ponte de l'albacore de l'Atlantique d'après les études du rapport gonado-somatique et des larves: résultats préliminaires. *Collect Vol Sci Pap* 5:94–100.
- Arocha, F., Lee, D., Marcano, L., Marcano, J. 2001. Update information on the spawning of yellowfin tuna, *Thunnus albacares*, in the Western Central Atlantic. *Collect Vol Sci Pap* 52:167–176.
- Ashton, W.D. 1972. The logit transformation with special reference to its uses in bioassay. 87 p. Hafner Pub. Co. Inc., New York.
- Bard, F.X., Capisano, C. 1991. Actualisation des connaissances sur la reproduction de l'albacore (*Thunnus albacares*) en océan Atlantique. *Recl Doc Sci* 36:158.
- Brown-Peterson, N.J., Wyanski, D.M., Saborido-Rey, F., et al. 2011. A standardized terminology for describing reproductive development in fishes. *Mar Coast Fish.* 3:52–70.
- Capisano, C., Fonteneau, A. 1991. Analyse des fréquences de longueur, du sex-ratio et des zones de reproduction de l'albacore, *Thunnus albacares*, de l'Atlantique. *Rec Doc Sci* 36:241–279.
- Caverivière, A. 1976. Longueur prédorsale, longueur a la fourche et poids des albacores (*Thunnus albacares*) de l'Atlantique. *Cah ORSTOM Sér Océan* 14:201–208.

- Chassot, E., Floch, L., Dewals, P., *et al.* 2015. Statistics of the French purse seine fishing fleet targeting tropical tunas in the Atlantic Ocean (1991-2013). *Collect Vol Sci Pap ICCAT* 71:540–572.
- Collette, B.B., and Naue, C.E. 1983. FAO species catalogue. Vol. 2: Scombrids of the world: an annotated and illustrated catalogue of tunas, mackerels, bonitos, and related species known to date. FAO Fish. Synop. 125, 137 p. FAO, Rome.
- Constance, D.N. 2015. Programme de renforcement des capacités du 04 au 18 juillet 2014 aux Seychelles rapport de la formation de perfectionnement: histologie des gonades de l'albacore et du patudo dans. *Collect Vol Sci Pap ICCAT* 71:434–439.
- Delgado, A.D., Floch, L., Rojo, V., *et al.* 2014. Statistics of the European and associated purse seine and baitboat fleets, in the Atlantic Ocean. *Collect Vol Sci Pap ICCAT* 70:2654–2668.
- Eveson, J.P., Million, J., Sardenne, F., Le Croizier, G. 2015. Estimating growth of tropical tunas in the Indian Ocean using tag-recapture data and otolith-based age estimates. *Fish Res* 163:58–68.
- Hunter, J., Macewicz, B. 1985. Rates of atresia in the ovary of captive and wild northern anchovy, *Engraulis mordax*. *Fish Bull* 83:119–136.
- Itano, D. 2000. The reproductive biology of yellowfin tuna (*Thunnus albacares*) in Hawaiian waters and the western tropical Pacific Ocean: project summary (p. 69). Hawaii: University of Hawaii, Joint Institute for Marine and Atmospheric Research.
- ICCAT. 2013. Rapport du Comité Permanent pour la Recherche et les Statistiques (SCRS). 375p
- ICCAT. 2011. Report for biennial period, 2010-11. Part II (2011) - Vol. 4 Rapport de la période biennale, 2010-11.
- Joseph, J. 2003. Managing fishing capacity of the world tuna fleet. FAO Fisheries Circular.
- Kell, L.T., Nash, R.D., Dickey-Collas, M., *et al.* 2015. Is spawning stock biomass a robust proxy for reproductive potential? *Fish and Fisheries*
- Marquardt, D.W. 1963. An algorithm for least-squares estimation of nonlinear parameters. *J Soc Ind Appl Math* 11:431–441.
- Marshall, C. 2009. Implementing information on stock reproductive potential in fisheries management: the motivation, challenges and opportunities. In: *Fish Reproductive Biology: Implications for Assessment and Management*. Wiley, p 395–420
- Marshall, C., Kjesbu, O., Yaragina, N., *et al.* 1998. Is spawner biomass a sensitive measure of the reproductive and recruitment potential of Northeast Arctic cod? *Can J Fish Aquat Sci* 55:1766–1783.
- McPherson, G.R. 1991. Reproductive biology of yellowfin tuna in the eastern Australian fishing zone, with special reference to the north-western Coral Sea. *Mar Freshw Res* 42:465–477.
- Morgan, M. 2008. Integrating reproductive biology into scientific advice for fisheries management. *J Northwest Atl Fish Sci* 41:37–51.
- Morgan, M., Murua, H., Kraus, G., *et al.* 2009. The evaluation of reference points and stock productivity in the context of alternative indices of stock reproductive potential. *Can J Fish Aquat Sci* 66:404–414.
- Murua, H., Motos, L. 2006. Reproductive strategy and spawning activity of the European hake *Merluccius merluccius* (L.) in the Bay of Biscay. *J Fish Biol* 69K1-F100:1288–1303.
- Murua, H., Saborido-Rey, F. 2003. Female reproductive strategies of marine fish species of the north Atlantic. *J Northw Atl Fish Sci* 33:23–31.

- Orange, C.J. 1961. Spawning of yellowfin tuna and skipjack in the eastern tropical Pacific, as inferred from studies of gonad development. *Inter-Am Trop Tuna Comm Bull* 5:457–526.
- Saborido-Rey, F., Junquera, S. 1998. Histological assessment of variations in sexual maturity of cod (*Gadus morhua* L.) at the Flemish Cap (north-west Atlantic). *ICES J Mar Sci J Cons* 55:515–521.
- Schaefer, K.M. 1998. Reproductive biology of yellowfin tuna (*Thunnus albacares*) in the eastern Pacific Ocean. *Inter-Am. Trop. Tuna Comm., Bull.* 21:205–221.
- Schaefer, K.M. 1996. Spawning time, frequency, and batch fecundity of yellowfin tuna, *Thunnus albacares*, near Clipperton Atoll in the eastern Pacific Ocean. *Fish Bull* 94:98–112.
- Stéquert, B., Ramcharrun, R. 1996. La reproduction du listao (*Katsuwonus pelamis*) dans le bassin ouest de l'océan Indien. *Aquat Living Resour* 9:235–247.
- Timohina, O.I., Romanov, E.V. 1996. Characteristics of ovogenesis and some data on maturation and spawning of skipjack tuna, *Katsuwonus pelamis* (Linnaeus, 1758), from the western part of the Equatorial Zone of the Indian Ocean.
- Trippel, E.A. 1999. Estimation of stock reproductive potential: history and challenges for Canadian Atlantic gadoid stock assessments. Variations in maturation, growth, condition and spawning stock biomass production in groundfish. *J Northwest Atl Fish Sci* Vol. 25:61–81.
- West, G. 1990. Methods of the assessing ovarian development in fishes: a review. *Aust J Mar Freshw Res* 41(2):199–222.
- Williams, E., Shertzer, K. 2003. Implications of life-history invariants for biological reference points used in fishery management. *Can J Fish Aquat Sci* 60:710–720.
- Zavala-Camin, L.A. 1977. Hipótesis sobre la estructura de población del rabil (*Thunnus albacares*), basada en el estudio de los estados de maduración sexual y de la frecuencia de tallas en ejemplares capturados en el sur del Brasil. *Collect Vol Sci Pap ICCAT* 6(1): 103–108.
- Zhu, G., Xu, L., Zhou, Y., Dai, X. 2008. Length-frequency compositions and weight length relations for bigeye tuna, yellowfin tuna, and albacore (Perciformes: Scombrinae) in the Atlantic, Indian, and eastern Pacific oceans. *Acta Ichthyol Piscat* 38:157–161.
- Zudaire, I., Murua, H., Grande, M., et al. 2013a. Fecundity regulation strategy of the yellowfin tuna (*Thunnus albacares*) in the Western Indian Ocean. *Fish Res* 138:80–88.
- Zudaire, I., Murua, H., Grande, M., Bodin, N. 2013b. Reproductive potential of yellowfin tuna (*Thunnus albacares*) in the western Indian Ocean. *Fish Bull* 111:252–264.



**Table 1.** Summary of the sampled individuals by 5 cm FL classes and by sex. Chi square test results are provided for size classes with more than 10 individuals.

<i>Size Class</i>	<i>Female</i>	<i>Male</i>	<i>Chis-Square</i>	<i>p-value</i>	
64-68	0	1	NA	NA	
69-73	0	1	NA	NA	
74-78	4	2	NA	NA	
79-83	8	3	2.2727	0.1317	
84-88	7	17	4.1667	0.04123	*
89-93	13	12	0.04	0.8415	
94-98	9	15	1.5	0.2207	
99-103	49	31	4.05	0.04417	*
104-108	90	106	1.3061	0.2531	
109-113	103	113	0.463	0.4962	
114-118	42	36	0.4615	0.4969	
119-123	32	41	1.1096	0.2922	
124-128	67	41	6.2593	0.01235	*
129-133	65	53	1.2203	0.2693	
134-138	60	36	6	0.01431	*
139-143	71	53	2.6129	0.106	
144-148	50	74	4.6452	0.03114	*
149-153	23	62	17.8941	2.34E-05	**
154-158	8	50	30.4138	3.49E-08	**
159-163	2	20	14.7273	0.0001242	**
164-168	1	5	NA	NA	
169-173	0	4	NA	NA	
>173	0	3	NA	NA	

\* $P < 0.05$       \*\* $P < 0.005$

**Table 2.** Summary of oocyte developmental stages in yellowfin tuna (YFT).

<i>Oocyte development stage</i>	<i>Characteristic</i>
<b>Primary growth</b>	
<i>Chromatin nuclear</i>	Oocyte is surrounded by a few squamous follicle cells. The nucleus is large and centrally located, surrounded by a thin layer of cytoplasm and containing a large and single nucleolus.
<i>Perinucleolar</i>	Nucleus increase in size and multiple nucleoli appear at its periphery. The “Balbiani bodies” migrated from the nucleus to the cytoplasm. At the end, some vacuoles appear in the cytoplasm and the chorion precursors material start to accumulate in patches.
<b>Cortical alveoli formation (CA)</b>	
	Spherical vesicles start to appear at the periphery of the cytoplasm. They increase in size and number forming rows and giving rise to cortical alveoli. Oil drops begin to accumulate in the cytoplasm. At this stage chorion and follicle layers are apparent.
<b>Vitellogenic (Vtg)</b>	
	This stage is characterized by the appearance of yolk vesicles in the cytoplasm. Besides, the separation of the chorion in two different layers occurred: inner and outer zona radiata. This stage is subdivided in 3 different stages.
<i>Vtg 1</i>	Oil droplets occupy more cytoplasmic area than yolk granules.
<i>Vtg 2</i>	Oil droplets occupy similar cytoplasmic area than yolk granules.
<i>Vtg 3</i>	Oil droplets occupy less cytoplasmic area than yolk granules.
<b>Oocyte Maturation (OM)</b>	
<i>Germinal Vesicle Migration (GVM)</i>	The nucleus (germinal vesicle) starts to migrate to the animal pole and the oil droplets fuse to coalescence into a unique oil globule.
<i>Germinal Vesicle Breakdown (GVBD)</i>	The nucleus completes its migration to the animal pole and the unique oil droplet is clearly evident at central part of the oocyte.
<i>Hydration</i>	Yolk granules fuse in yolk plates, and eventually form a homogeneous mass. The nucleus has disintegrated and the cortical alveoli and cytoplasm are restricted to a thin peripheral layer. The oocyte significantly increases in size due to the uptake of fluids. Hydrated oocyte has a translucent appearance.

**Table 3.** Summary of the number of individuals sampled by 5-cm  $F_L$  classes and maturity development for female yellowfin tuna (YFT). See **Table 1** for definitions of oocyte development stages.

$F_L$	<i>IP</i>	<i>DP</i>				<i>SCP</i>				<i>RsP</i>	<i>RgP</i>	<i>Total</i>
	<i>PG</i>	<i>CA</i>	<i>V1</i>	<i>V2</i>	<i>V3</i>	<i>GVM</i>	<i>GVBD</i>	<i>HYD</i>				
74-78	4											4
79-83	5	3										8
84-88	6	1										7
89-93	7	1	1							1		10
94-98	5	2										7
99-103	17	15		1						1		34
104-108	21	32	3							1	2	59
109-113	20	18	6			1	1		1	12	4	63
114-118	7	14	3	2		1				4	5	36
119-123	3	7	2			1				8	4	25
124-128	2	13	5	5		7	1	2	5	8	4	52
129-133	1	6	2	10		11	4	2	2	5	5	48
134-138			1	10		13	2	2	10	2	2	42
139-143		1	3	7		11	3	6	23		1	55
144-148			1	8		11		6	12	4	1	43
149-153			1	4		5	1	3	5	4		23
154-158				1		1		1	2	3		8
159-163						1		1				2
164-168				1								1
<b>Total</b>		<b>98</b>	<b>113</b>	<b>28</b>	<b>49</b>	<b>63</b>	<b>12</b>	<b>23</b>	<b>60</b>	<b>53</b>	<b>28</b>	<b>527</b>

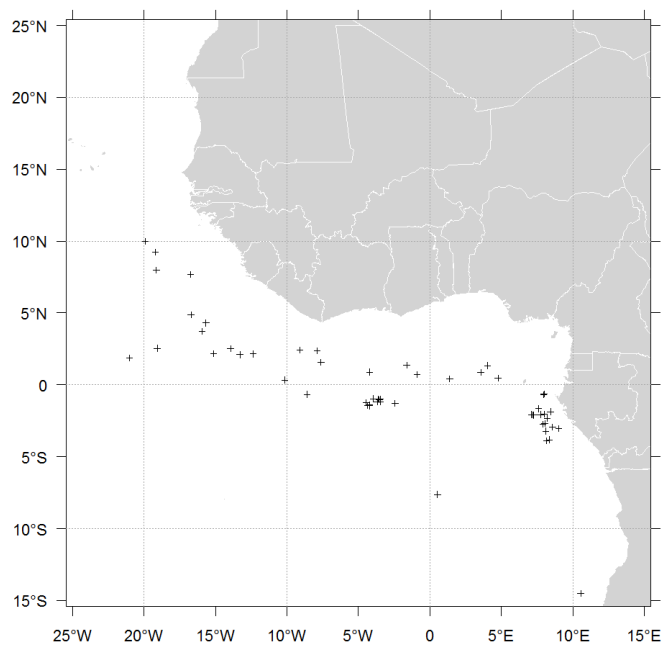


**Figure 1.** Fishing areas of the yellowfin tuna (YFT) caught by purse seiners in this study.

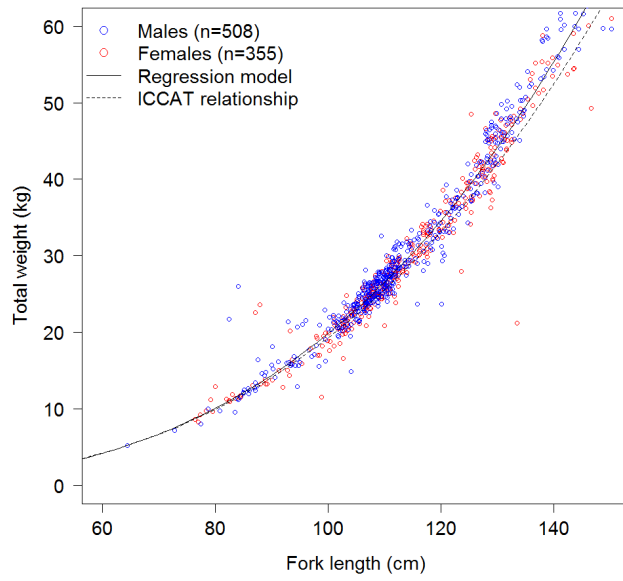


**Figure 2.** Relationship between fork length ( $F_L$ , cm) and body weight (kg) for male and female yellowfin tuna (YFT) sampled in the cannery of the fishing port of Abidjan from February 2014 to February 2015.

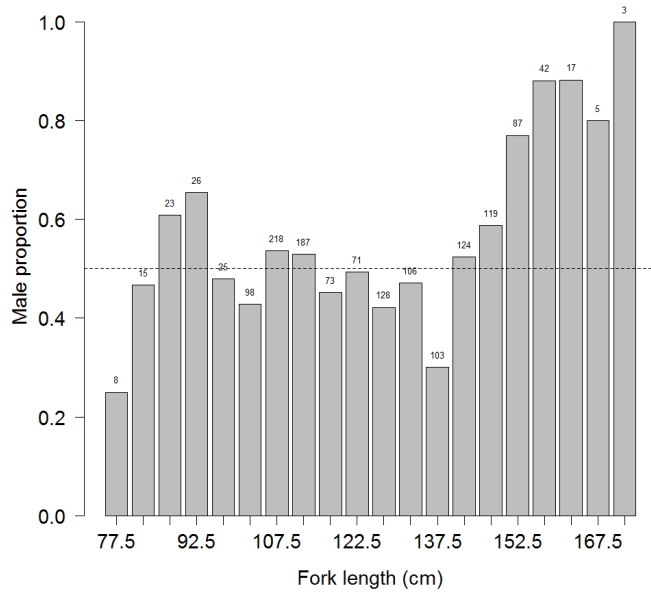


**Figure 3.** Monthly variations of sex-ratio of yellowfin tuna (YFT) in the Eastern Atlantic Ocean.

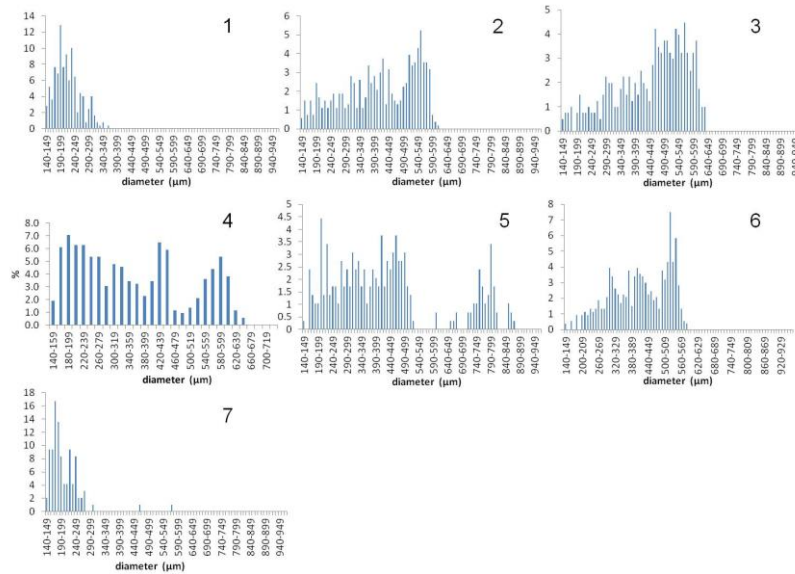


**Figure 4.** Relative oocyte size-frequency distribution for each ovarian development phase, from developing phase to regenerating phase ovaries, in yellowfin tuna (YFT) from the Eastern Atlantic Ocean. 1-2 Developing phase, 3-5 Spawning capable phase, 6 Regressing phase, and 7 Regenerating phase.

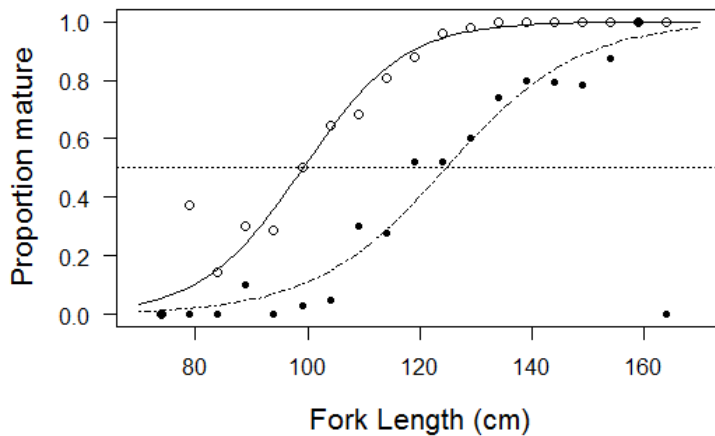


**Figure 5.** Proportion of mature female YFT in the Eastern Atlantic Ocean at 5-cm  $F_L$  intervals. White circles represent the proportions of females considered mature when their ovaries were at the cortical alveolar stage and onward; the grey solid line indicates the logistic regression curve fitted to the data. Black circles represent the proportions of females considered mature when their ovaries were at the vitellogenic stage and onward; the dark solid line indicates the logistic regression curve fitted to these data. The horizontal dotted line indicates  $L_{50}$ , i.e. the length at which 50% of the female yellowfin tuna (YFT) population was mature.

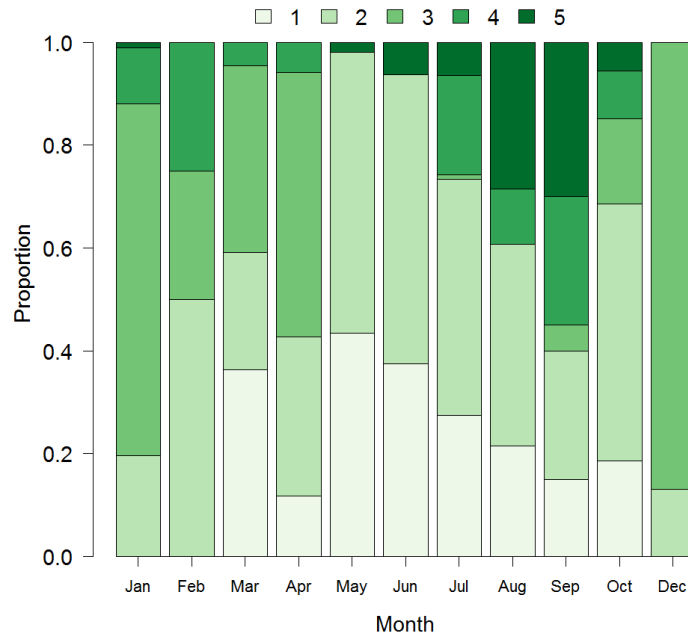


**Figure 6.** Monthly proportion of ovary development phases (1 = Immature phase; 2 = Developing phase; 3 = Spawning capable phase; 4 = Regressing phase; 5 = Regenerating phase) for female yellowfin tuna (YFT).

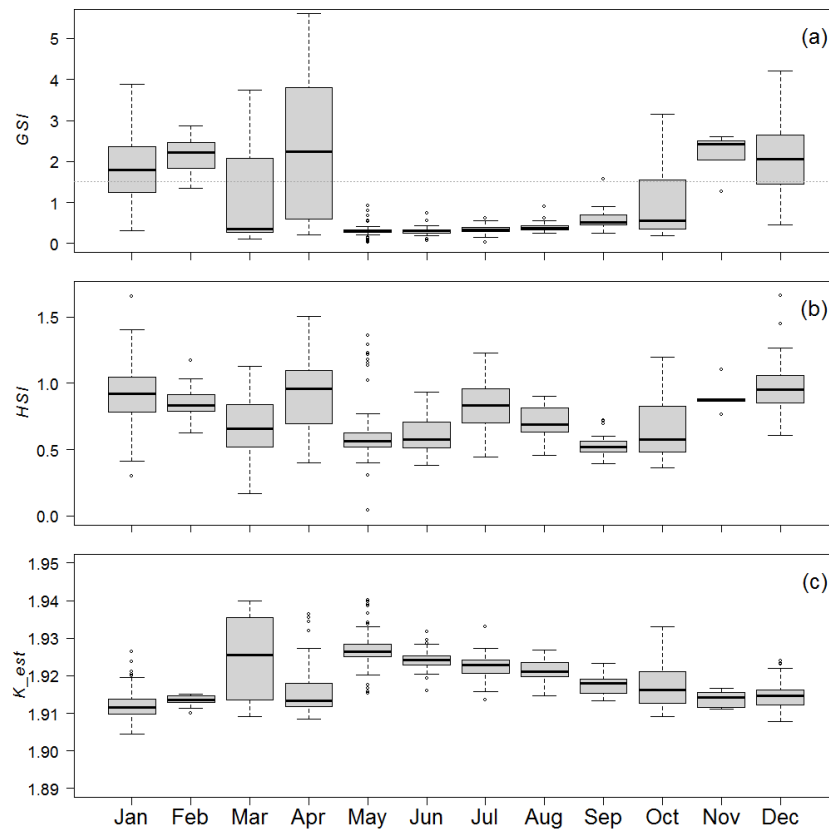


**Figure 7.** Seasonal variation of (a) gonado-somatic index  $GSI$ , (b) hepato-somatic index  $HSI$  and (c) condition index  $K$  for female yellowfin tuna (YFT) caught with purse seine in the Eastern Atlantic Ocean.

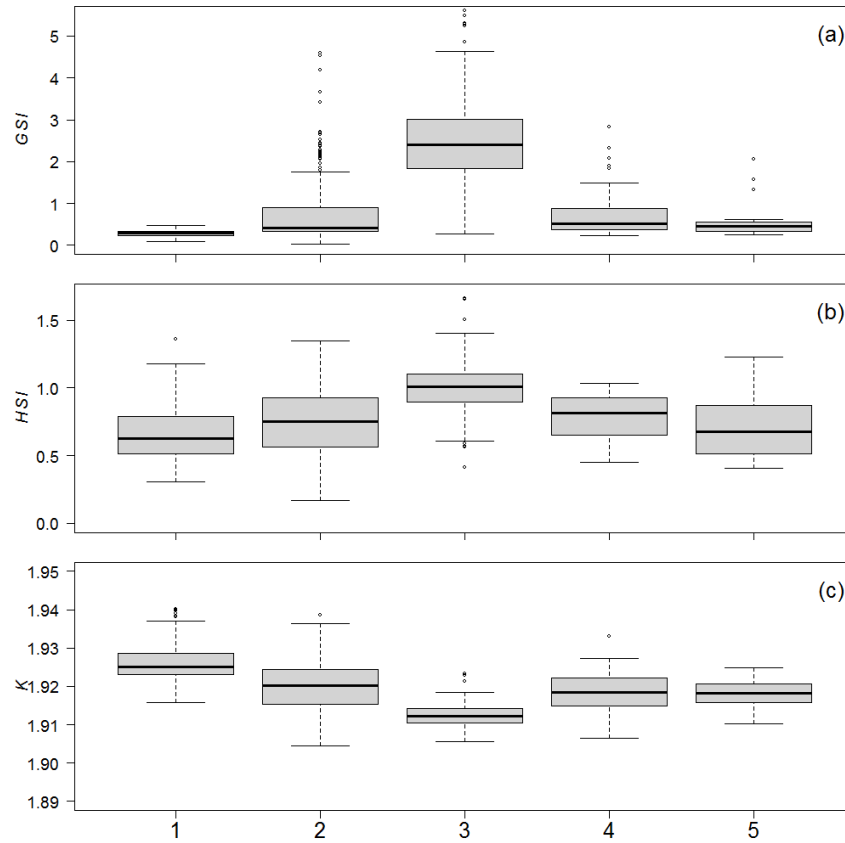


**Figure 8.** Variation of (a) gonadosomatic index *GSI*, (b) hepatosomatic index *HSI* and (c) condition index *K* according to the ovarian development stages for female yellowfin tuna (YFT) caught with purse seine in the Eastern Atlantic Ocean. 1 = Immature phase; 2 = Developing phase; 3 = Spawning capable phase; 4 = Regressing phase; 5 = Regenerating phase.